Biochimica et Biophysica Acta 1838 (2014) 2745–2756

Contents lists available at ScienceDirect

Biochimica et Biophysica Acta

journal homepage: www.elsevier.com/locate/bbamem

I–J loop involvement in the pharmacological profile of CLC-K channels expressed in *Xenopus* oocytes

Antonella Gradogna [a], Paola Imbrici [b], Giovanni Zifarelli [a], Antonella Liantonio [b], Diana Conte Camerino [b], Michael Pusch [a,*]

[a] Istituto di Biofisica, CNR, Via De Marini 6, 16149 Genoa, Italy
[b] Dipartimento di Farmacia-Scienze del farmaco, Università degli Studi di Bari, Via Orabona 4, 70125 Bari, Italy

ARTICLE INFO

Article history:
Received 20 March 2014
Received in revised form 13 July 2014
Accepted 21 July 2014
Available online 26 July 2014

Keywords:
Chloride channels
CLC-Ka
CLC-K1
Niflumic acid

ABSTRACT

CLC-K chloride channels and their subunit, barttin, are crucial for renal NaCl reabsorption and for inner ear endolymph production. Mutations in CLC-Kb and barttin cause Bartter syndrome. Here, we identified two adjacent residues, F256 and N257, that when mutated hugely alter in *Xenopus* oocytes CLC-Ka's biphasic response to niflumic acid, a drug belonging to the fenamate class, with F256A being potentiated 37-fold and N257A being potently blocked with a $K_D \sim 1$ μM. These residues are localized in the same extracellular I–J loop which harbors a regulatory Ca^{2+} binding site. This loop thus can represent an ideal and CLC-K specific target for extracellular ligands able to modulate channel activity. Furthermore, we demonstrated the involvement of the barttin subunit in the NFA potentiation. Indeed the F256A mutation confers onto CLC-K1 a transient potentiation induced by NFA which is found only when CLC-K1/F256A is co-expressed with barttin. Thus, in addition to the role of barttin in targeting and gating, the subunit participates in the pharmacological modulation of CLC-K channels and thus represents a further target for potential drugs.

1. Introduction

CLC-K channels belong to the family of CLC proteins that is responsible for transepithelial and intracellular Cl^- transport in several tissues and organs. So far four isoforms have been electrophysiologically characterized: human CLC-Ka/CLC-Kb and the rodent (rat and mouse) CLC-K1 [1–3]. CLC-K channels are expressed in the kidney [1,2,4] and in the inner ear [5] where they are involved in NaCl reabsorption [6] and in the production of the endolymph [7,8], respectively. They co-localize with the β-subunit, barttin [5], a small protein that affects CLC-K trafficking, stability, and gating by unknown mechanisms [5,9–12]. CLC-K channels are modulated by external Ca^{2+} and pH. CLC-K currents increase by increasing $[Ca^{2+}]_{ext}$, while they are blocked by external acidification or extreme alkalinization [4,5,13–15]. The association of loss of function mutations of CLC-Kb and barttin with Bartter syndrome, types III and IV respectively [9,16], and the proposal that gain of function mutations may favor hypertension [17,18] encouraged studies aimed to identify CLC-K activators and inhibitors. By a detailed pharmacological investigation performed on CLC-K channels expressed in *Xenopus* oocytes, CPP derivatives, DIDS and flufenamic acid, an anti-inflammatory drug belonging to the class of fenamates, were found to inhibit CLC-Ka [19–23]. Interestingly, niflumic acid (NFA), another member of the same class of fenamates, is the most potent CLC-K opener so far identified [19,24,25]. Each CLC-K isoform shows a different response to extracellular NFA: $[NFA]_{ext} \leq 0.5$ mM increases CLC-Ka currents whereas higher concentrations block this channel [19]; hCLC-Kb is potentiated by $[NFA]_{ext}$ up to 2 mM [19]; and rat CLC-K1 is blocked at all concentrations tested [24]. The biphasic NFA action on CLC-Ka has been explained by two separate binding sites for NFA that are involved in the block and potentiation of the channel, respectively [19]. These binding sites are distinct from that known for CPP derivatives and FFA [24]. By a mutagenic screen on CLC-Ka three residues (L155, G345, A349) were identified that when mutated decreased NFA potentiation and could thus participate in the potentiating binding site or be involved in conformational changes associated with potentiation [25]. Surprisingly, NFA no longer potentiated currents of hCLC-Ks expressed in mammalian cells [26]. In order to identify the molecular determinants of CLC-K activation, here we further investigated NFA potentiation of CLC-Ks in oocytes, the model system where hCLC-K potentiation was found. A further incentive for our study came from the identification of four acidic residues, located in (or close to) the I–J loop of the channel, that form an intersubunit Ca^{2+} binding site [14,27]. The I–J loop connects the two halves with opposite orientation (B–I and J–Q) of a CLC monomer [28]. Since Ca^{2+} regulation is found only in CLC-Ks among CLC proteins, we hypothesized that the I–J loop might be involved in the channel

Abbreviations: CPP, p-chloro-phenoxy-propionic acid; DIDS, diisothiocyanato-2,2′-stilbenedisulfonic acid; NFA, niflumic acid; FFA, flufenamic acid; CPA, p-chlorophenoxy-acetic acid

* Corresponding author. Tel.: +39 0106475 330/522; fax: +39 0106475 500.
E-mail address: pusch@ge.ibf.cnr.it (M. Pusch).

http://dx.doi.org/10.1016/j.bbamem.2014.07.021

modulation by other extracellular ligands. Indeed, we identified two adjacent residues of the I–J loop, F256 and N257, that when mutated alter NFA potentiation. Mutant F256A dramatically increases the NFA activation of CLC-Ka whereas N257A is only blocked by NFA with high affinity. Using CLC-K1, which shows functional expression also without barttin, we demonstrated the involvement of barttin in CLC-K potentiation by NFA. Finally, the F256A CLC-Ka mutant partially recovered the biphasic NFA response of CLC-Ka expressed in HEK293 cells, confirming F256 involvement in the potentiation by NFA. F256, N257 and three of the residues forming the Ca^{2+} binding site are localized in the I–J loop. Thus, this loop represents an interesting pharmacological target for extracellular CLC-K ligands.

2. Materials and methods

2.1. Molecular biology

Mutations were inserted by recombinant PCR as described previously [29].

For expression in *Xenopus* oocytes: after linearization, cRNA of CLC-K channels and barttin subunit were transcribed by mMessage mMachine SP6 kit and T7 RNA polymerase (Ambion), respectively. CLC-K constructs were co-expressed with barttin mutant Y98A [5], except CLC-K1 constructs that could be expressed also by themselves.

For the CLC-K expression in HEK293 cells: F256A CLC-Ka and barttin constructs were subcloned in the pcDNA3 vector.

2.2. Electrophysiology

After cRNA injection [23], oocytes were kept at 18 °C in the maintaining solution containing (in mM): 90 NaCl, 2 KCl, 1 $MgCl_2$, 1 $CaCl_2$, and 10 Hepes at pH 7.5. One to three days after injection voltage clamp measurements were performed by using the custom acquisition program GePulse (available at http://users.ge.ibf.cnr.it/pusch/programs-mik.htm) and a Turbo TEC-03X amplifier (npi electronic, Tamm, Germany). The standard bath solution contained (in mM): 90 NaCl, 10 $CaCl_2$, 1 $MgCl_2$, and 10 Hepes at pH 7.3 (osmolarity: 190 mosm). Different NFA concentrations were prepared immediately before use by diluting niflumic acid that was dissolved in dimethyl sulfoxide (DMSO) in the standard bath solution. Final [DMSO] was ≤0.2%. The holding potential was kept at ~−30 mV corresponding to the resting membrane potential in our conditions. To estimate CLC-K currents at different potentials, the "IV-pulse protocol" was applied: a prepulse to −100 mV for 100 ms was followed by voltages ranging from −140 to 80 mV with 20 mV increments for 200 ms. Pulses ended with a tail to 60 mV for 100 ms. Interpulse duration was 1.5 s. The effect of $[NFA]_{ext}$ was monitored by applying 200 ms pulses to 60 mV once per second. To estimate endogenous and leak currents a solution containing (in mM): 100 NaI, 5 $MgSO_4$, and 10 Hepes at pH 7.3 was applied [22].

HEK293 cells were co-transfected with three plasmids encoding F256A CLC-Ka, barttin, and GFP, respectively. The latter allowed the identification of transfected cells by their fluorescence. Two to three days after transfection, whole-cell patch-clamp recordings were performed. Pipettes were pulled from borosilicate glass capillaries (Hilgenberg, Malsfeld, Germany) and had resistances of 2.0–2.7 MΩ in the recording solutions. Experiments in which series resistance led to voltage errors larger than a few mV were discarded. The extracellular standard bath solution contained (in mM): 145 NaCl, 2 $CaCl_2$, 2 $MgCl_2$, and 10 Hepes at pH 7.3 (osmolarity: 277 mOsm). The intracellular solution contained (in mM): 130 CsCl, 2 EGTA, 2 $MgCl_2$, and 10 Hepes at pH 7.3 (osmolarity 233 mOsm). F256A CLC-Ka currents were assayed with the following stimulation protocol: after a prepulse to 60 mV for 20 ms, channels were stimulated with potentials ranging from −140 to 80 mV with 20 mV increments for 200 ms. Pulses ended with a tail pulse to 80 mV for 50 ms. Holding potential was 0 mV. To evaluate the effect of NFA, CLC-Ks were stimulated with repetitive 10 ms pulses to 60 mV delivered once per second. Leak currents were evaluated applying a solution that blocks specifically CLC-Ks [22] containing (in mM): 140 NaI, 2 $CaCl_2$, 2 $MgSO_4$, and 10 Hepes at pH 7.3.

2.3. Data analysis

Currents recorded at different $[NFA]_{ext}$ were normalized to the steady state currents measured at 60 mV in control conditions. Normalized

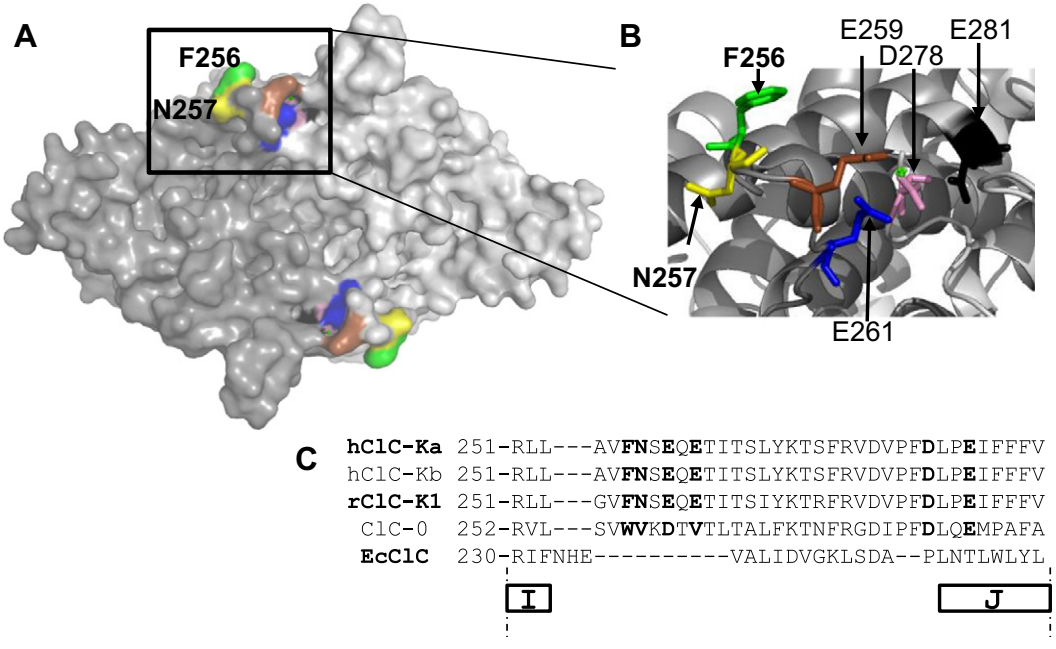

Fig. 1. Localization of F256 and N257 and of the Ca^{2+} binding site on the homology model of CLC-Ka. (A) Surface representation of the CLC-Ka model [27]. The two subunits viewed from the extracellular side are indicated by two tones of gray. The residues involved in the response to NFA (F256 and N257) and those that coordinate Ca^{2+} (E259, E261, D278, E281) [14,27] are colored differently: green F256, yellow N257, red E259, blue E261, pink D278, and black E281. (B) Zoom of the region containing the residues of interest. Residues are depicted as sticks and colored as in A. (C) Sequence alignment around the I–J loop of CLC-Ka, -Kb, -K1, CLC-0, and EcCLC.

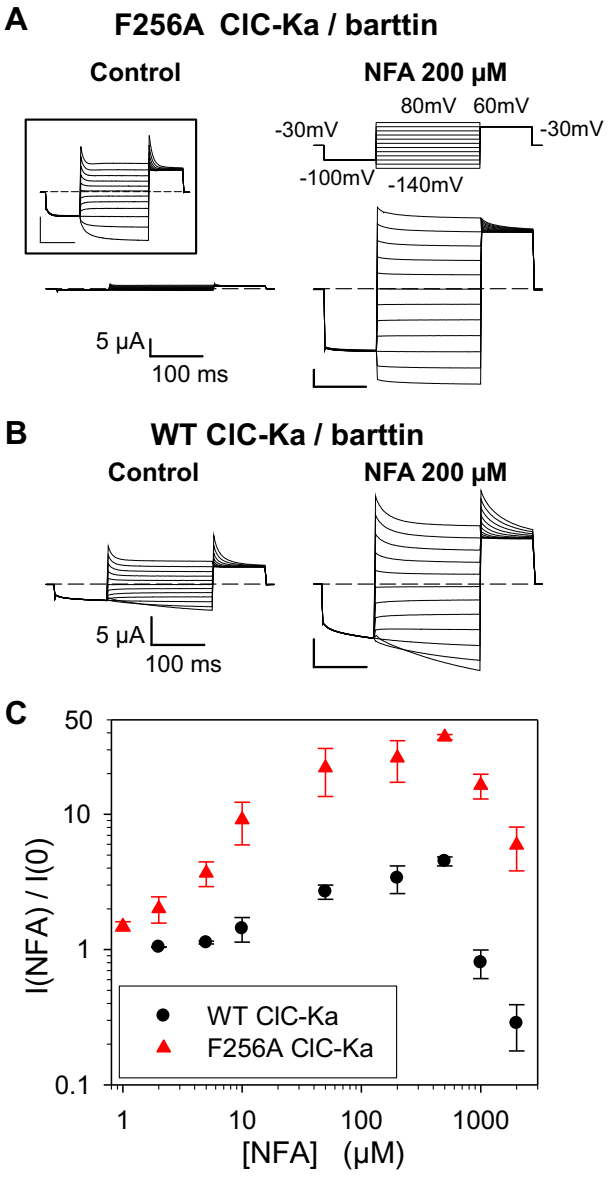

Fig. 2. F256A CLC-Ka is hugely activated by NFA. (A–C) Effect of NFA on F256A and WT CLC-Ka in *Xenopus* oocytes. Typical currents of F256A (A) and WT CLC-Ka (B) in response to the IV-protocol (top) in control (left) and at 200 μM NFA (right). The inset (A) shows F256A currents at high magnification (C) Dose–response relationship of NFA modulation of WT and F256A CLC-Ka. The currents acquired at 60 mV are normalized to values measured in standard solution (i.e. 0 NFA) and plotted versus $[NFA]_{ext}$ (used concentrations: 1, 2, 5, 10, 50, 200, 500, 1000 and 2000 μM) ($n \geq 3$).

currents were plotted versus $[NFA]_{ext}$. Leak currents were subtracted. Error bars indicate SD.

2.4. Noise analysis

Patch-clamp measurements were performed in the inside-out configuration on *Xenopus* oocytes. The intracellular (bath) solution contained (in mM): 100 N-methyl-D-glucamine-Cl (NMDG-Cl), 2 $MgCl_2$, 2 EGTA, and 10 Hepes at pH 7.3. The extracellular (pipette) solution contained (in mM): 90 N-methyl-D-glucamine-Cl (NMDG-Cl), 10 $CaCl_2$, 1 $MgCl_2$, and 10 Hepes at pH 7.3. To estimate the effect of NFA on F256A and N257A CLC-Ka 200 and 4 μM NFA were dissolved in extracellular solution, respectively. In the experiments with F256A CLC-Ka an intracellular solution in which Cl^- was replaced by glutamate was used to evaluate endogenous and leak currents; the same aim was obtained

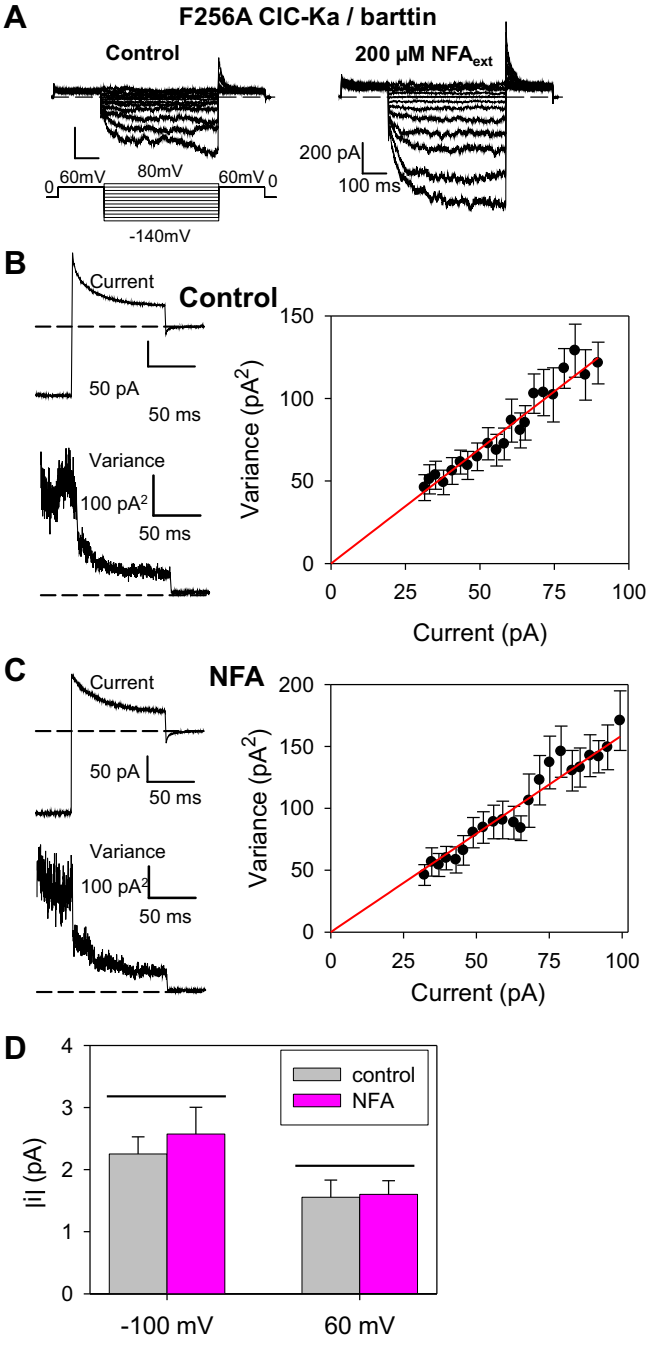

Fig. 3. Non-stationary noise analysis of F256A CLC-Ka. (A) Typical current traces recorded by patch clamp in configuration inside-out from different oocytes without NFA (left) and with 200 μM NFA_{ext} (right) evoked by the stimulation protocol (bottom). (B–C) Examples of non-stationary noise analysis of F256A CLC-Ka in standard conditions (B) and in the presence of 200 μM NFA_{ext} (C) at 60 mV. (left). Mean currents (upper) and variance (lower) are shown as a function of time. Right: Variance (symbols) is plotted versus the mean current and fitted with a parabola (red line) as described in the Materials and methods section. (D) Bars represent the absolute value of the single channel mean current in control solution and at 200 μM NFA_{ext} at two different potentials (−100 mV and 60 mV) ($n \geq 4$), $p > 0.2$ (unpaired Student's t-test) (background variance and leak currents were subtracted).

in the experiments on N257A CLC-Ka by using an intracellular solution in which 2 mM CPA (p-chlorophenoxy-acetic acid) was dissolved. Patch pipettes were pulled from aluminosilicate glass capillaries (Hilgenberg, Malsfeld, Germany) and had resistances of 0.8–1.5 MΩ in the recording solutions. F256A and N257A CLC-Ka currents were assayed with the following stimulation protocol: after a prepulse to 60 mV for 200 ms,

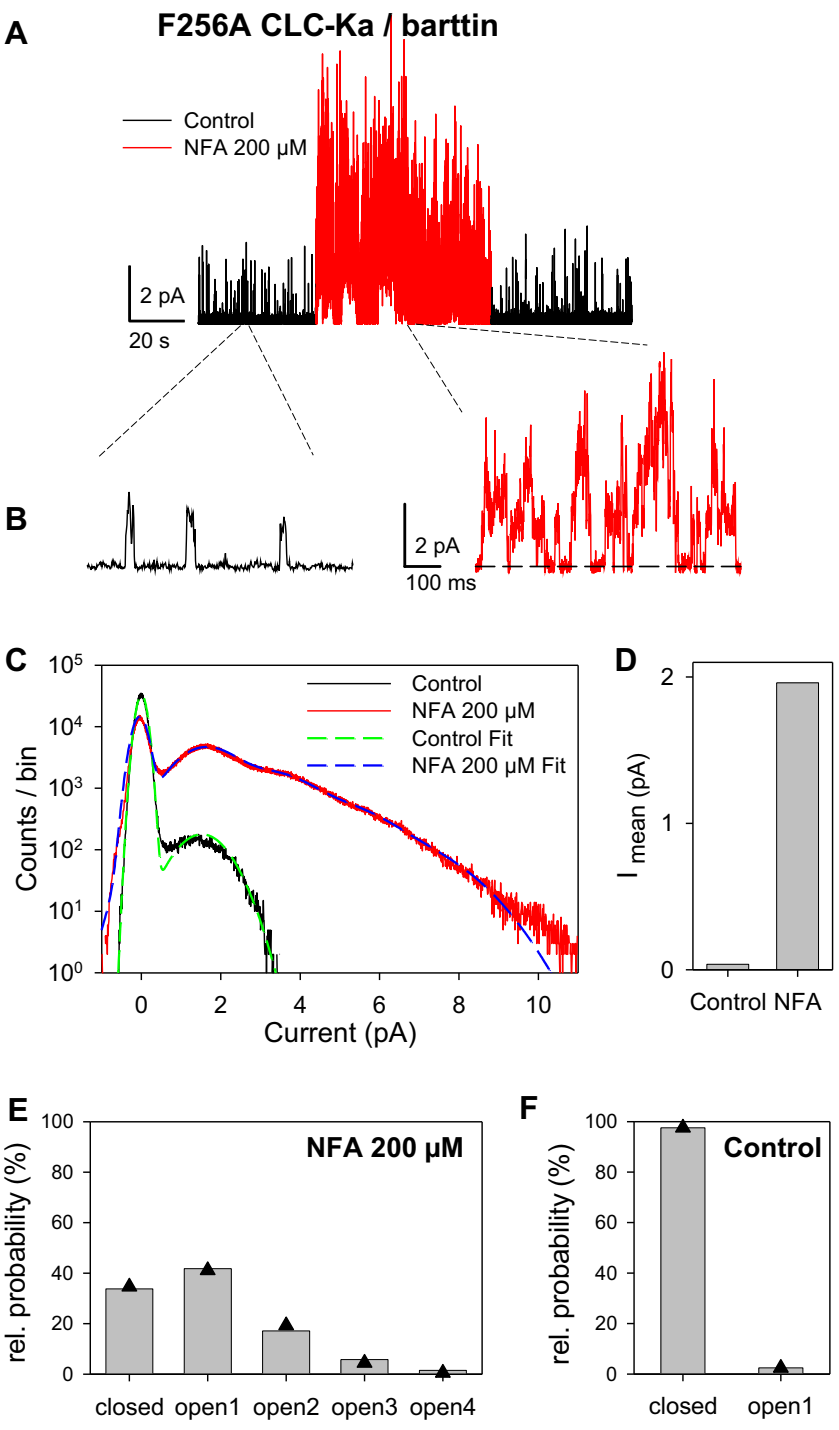

Fig. 4. NFA increases the open probability of F256A CLC-Ka. Example of single channel recordings and analysis from a single patch (similar experiments allowing the estimation of the number of channels: n = 3; 2 additional patches with larger currents were allowed to estimate the degree of potentiation but not the number of channels). (A) Continuous recording from F256A CLC-Ka at 60 mV. Different colors represent the external solutions applied during the experiment (black: control, red: 200 μM NFA). (B) Portions of the recording in (A) shown at higher time resolution. (C) The amplitude histogram of the recording at 60 mV in control solution (black trace) and in the presence of 200 μM NFA (red trace). Fit curves are superimposed as dashed lines. (D) Mean current from the recording in (A) measured at 60 mV for 40 s in control solution and in 200 μM NFA. (E–F) Probabilities of the conductance states in 200 μM NFA and in control solution. The measured state probabilities are shown as bars, whereas the symbols are the expected values from the binomials fits (see the Materials and methods section) resulting in N = 5 channels, p = 20% in NFA and p = 0.3% in control (for the fit in control, the number of channels was fixed to 5, as obtained in the presence of NFA).

channels were stimulated with potentials ranging from −140 to 80 mV with 20 mV increments for 500 ms. Pulses ended with a tail pulse to 60 mV for 200 ms. To estimate the single-channel current by non-stationary noise analysis the following stimulation protocol was applied 100–200 times: a prepulse to 60 mV was followed by a pulse to −100 mV for 300 ms. Pulses ended with a tail at 60 mV for 200 ms. Currents were recorded at 50 kHz after filtering at 10 kHz with an eight-pole Bessel filter. An intracellular solution in which 100 μM CPA was dissolved was used for the measurements on N257A CLC-Ka to induce current relaxations. Data analysis was performed at −100 mV and 60 mV; holding potential was 0 mV. First the mean current, I was calculated. The variance, σ^2, was estimated from the averaged squared difference of consecutive traces

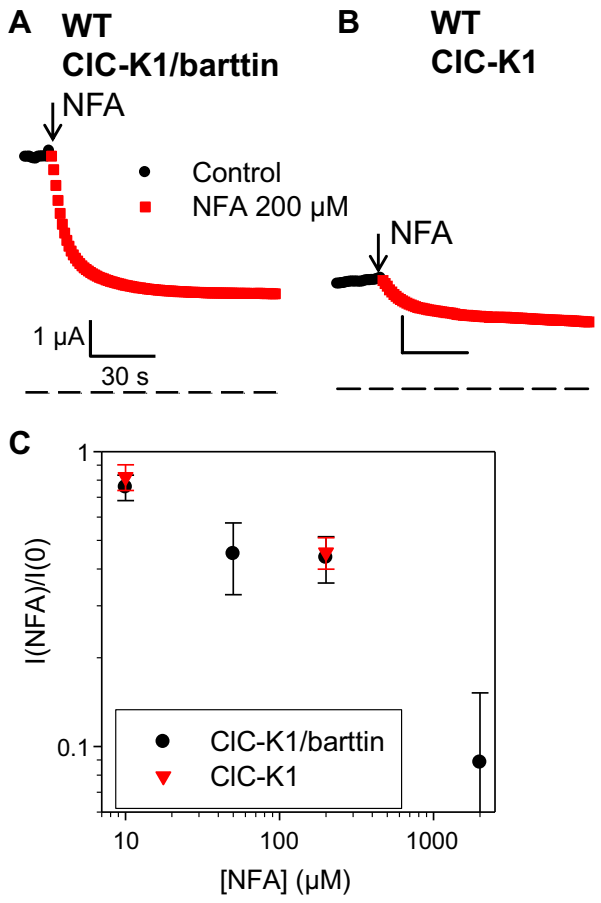

Fig. 5. WT CLC-K1 is blocked by NFA both with and without barttin. Effect of 200 μM NFA on WT CLC-K1/barttin (A) and WT CLC-K1 (B). Currents are plotted as function of the time. Colors and symbols correspond to the different solutions applied during the experiment. (C) Dose response of NFA effect on WT CLC-K1 with and without barttin. Currents normalized to those recorded in standard solution are plotted versus $[NFA]_{ext}$ (concentrations tested on CLC-K1/barttin: 10, 50, 200, 2000 μM, n ≥ 3; concentrations tested on CLC-K1: 10, 200 μM, n ≥ 3).

subtracting the background variance at 0 mV. The variance–mean plot was assembled by binning as described previously [30]. Finally the variance–mean plot was fitted by $\sigma^2 = iI - I^2 / N$, with the single channel current, *i*, and the number of channels, *N*, as free parameters [31].

2.5. Single channel analysis

Single channel measurements were performed on *Xenopus* oocytes in outside-out and inside-out configuration to study the effect of extracellular NFA on F256A CLC-Ka and intracellular CPA on N257A CLC-Ka, respectively. The intracellular solution was the same as used for the noise analysis. For the outside-out recordings, the extracellular solution contained (in mM): 92 tetraethylammonium chloride (TEA-Cl), 10 $CaCl_2$, and 10 Hepes at pH 7.3. Pipettes were pulled from borosilicate glass capillaries (Hilgenberg, Malsfeld, Germany) and had resistances of 9–10 MΩ in the recording solution. The outside-out recordings of F256A were performed at 60 mV in continuous local perfusion switching between control and NFA containing external solution. For the inside-out experiments of N275A, the extracellular solution contained (in mM): 92 N-methyl-D-glucamine-Cl (NMDG-Cl), 10 $CaCl_2$, and 10 Hepes at pH 7.3 and pipettes had resistances of 3–4 MΩ in the recording solution. Inside-out recordings of N257A were performed at −100 mV in continuous perfusion with intracellular solution with or without CPA. Currents were filtered at 3 kHz and sampled at 50 kHz. Single channel analysis was performed as described by Ludewig et al. [32]. Briefly, after digital filtering at 600 Hz, amplitude histograms were manually fitted by Gaussian functions using custom software. The respective area of each Gaussian component was used to calculate the open probability, p(k), of each conductance state k (k = 0 refers to the baseline). These were used to obtain the number of channels and the open probability by optimizing the parameters N and p in the following equation, describing a binomial distribution:

$$p(k) = \binom{N}{k} p^k (1-p)^{N-k}.$$

3. Results

3.1. The F256A mutation hugely increases CLC-Ka potentiation by NFA in Xenopus oocytes

The identification of an intersubunit Ca^{2+} binding site in the I–J loop [14,27] (Fig. 1A–C) motivated us to investigate if the I–J loop might be involved also in the channel modulation by NFA. We identified two adjacent, externally exposed residues, F256 and N257 (Fig. 1A, B), that when mutated dramatically changed the CLC-Ka response to NFA. F256A CLC-Ka expressed in *Xenopus* oocytes yields currents similar to those of WT regarding both kinetics and magnitude (Fig. 2A inset). However, at 200 μM NFA F256A and WT currents increase ~25-fold (Fig. 2A) and 3-fold (Fig. 2B), respectively. The activating effect of NFA was so marked that F256A currents in the absence of NFA had to be <1 μA to avoid series resistance problems after adding NFA (Fig. 2A, left). Both WT and F256A CLC-Ka show maximal stimulation at 500 μM NFA (4-fold and 37-fold, respectively) (Fig. 2C). However the F256A mutant is potentiated by NFA at all the concentrations tested (from 1 to 2000 μM) (Fig. 2C) with a two-fold potentiation already at 2 μM. Instead WT currents are not changed by very low $[NFA]_{ext}$ and are inhibited by $[NFA]_{ext}$ > 500 μM (Fig. 2C). The less pronounced potentiation at high $[NFA]_{ext}$ indicates that potentiation and block coexist also for this mutant as for WT (Fig. 2C). An important question is whether NFA affects directly the ion permeation or whether it acts indirectly modifying the open probability of F256A CLC-Ka. By using patch-clamp experiments in the inside-out configuration and non-stationary noise analysis we estimated the single channel current without and with NFA (Fig. 3). NFA does not change the current kinetics of F256A CLC-Ka (Fig. 3A). By repetitive pulses to 60 mV after a prepulse to −100 mV mean current and variance (Fig. 3B and C, left) were estimated. The single channel current was estimated from the fit of a parabola to the variance–mean plot (Fig. 3B and C, right), as described in the Materials and methods section. The fact that the variance–mean plots in control as well as in the presence of NFA showed no sign of curvature suggests that even after the dramatic potentiation by NFA the open probability of the F256A mutant is significantly below 0.5, and impossible to estimate from this analysis. Importantly, both at negative and positive potentials, 200 μM NFA does not change significantly the conductance of F256A CLC-Ka (Fig. 3D). This suggests that an allosteric increase of open probability is responsible for NFA effect on F256A CLC-Ka. To confirm this hypothesis we performed single channel recordings in the outside-out configuration (Fig. 4). Fig. 4A shows a typical recording. In the absence of NFA channel activity is low, showing a single open conductance level of ~1.6 pA (average: 1.55 ± 0.06 pA (n = 3)) (Fig. 4A, B left, C), in agreement with the noise analysis. Channel openings are very flickery as evidenced by a large width of the corresponding Gaussian component (Fig. 4C). Application of 200 μM NFA immediately (within the time of a few seconds needed to change the solution) dramatically increases the mean current in the patch about 53-fold (Fig. 4D) (average current increase: 39 +/− 13 (SD); n = 5 patches). Interestingly, the potentiation is quickly reversed upon washout of NFA (Fig. 4A) demonstrating that it does not reflect an increase of the number of channels present in the patch. Qualitatively, the multiple conductance levels

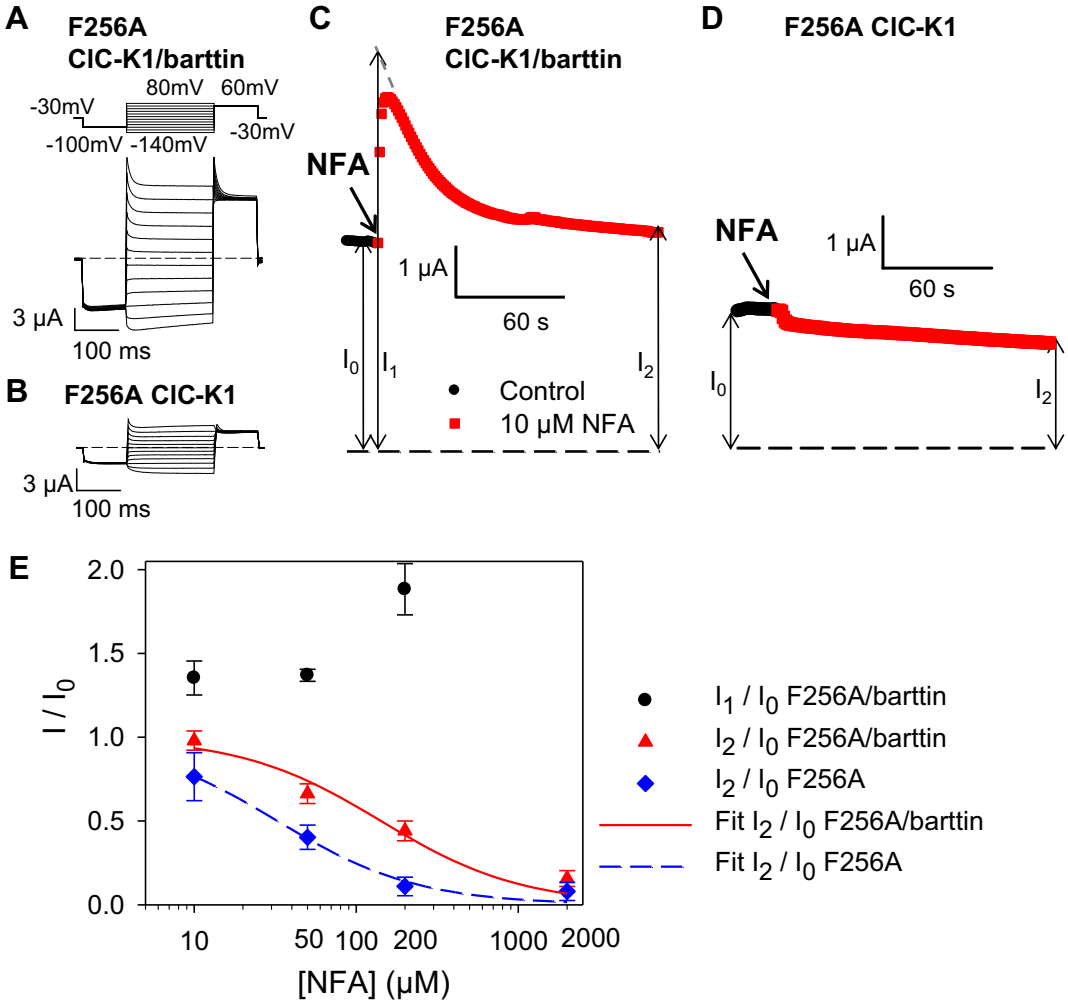

Fig. 6. Barttin involvement in the potentiation of F256A CLC-K1. Voltage-clamp traces of F256A CLC-K1/barttin (A) and F256A CLC-K1 (B) evoked by the IV-protocol in standard solution. (C–E) NFA effect on F256A CLC-K1 expressed with barttin or by itself in *Xenopus* oocytes. Current of F256A CLC-K1/barttin (C) and F256A CLC-K1 (D) at 60 mV is shown as function of time. Colors and symbols correspond to the solutions applied. Vertical arrows indicate the initial current (I_0), the maximal NFA potentiation extrapolated by a single-exponential function (I_1), and the steady state current (I_2). (E) Dose–response relationship of NFA potentiation of F256A/barttin CLC-K1 and NFA inhibition of F256A CLC-K1/barttin and F256A CLC-K1. I_1/I_0 and I_2/I_0 are plotted versus $[NFA]_{ext}$ (used concentrations: 10, 50, 200, and 2000 µM, $n \geq 3$). The lines represent the fit curves obtained from the equation $I_2 / I_0 = 1 / (1 + (c / K_D))$ for NFA block of F256A/barttin (K_D ~ 142 µM) and F256A (K_D ~ 33 µM).

seen in NFA (Fig. 4B, right) are consistent with an unchanged single channel conductance. This is confirmed by the analysis of the amplitude histogram (Fig. 4C), which can be well fitted by the superposition of roughly equally spaced Gaussian components with a distance of 1.8 pA, again in good agreement with the noise analysis and demonstrating that NFA has almost no effect on the single channel conductance (average: 1.75 ± 0.10 pA (n = 3) in NFA). Importantly, the amplitude histogram analysis allows to obtain an estimate of the absolute open probability of mutant F256A. For the patch shown in Fig. 4, in the presence of NFA, the occupation probabilities of the various conductance levels obtained from the Gaussian fit (Fig. 4E, bars) can be well fitted (see the Materials and methods section) assuming the presence of 5 independent and identical channels each having an open probability of p_{NFA} = 20% (Fig. 4E, triangles). Assuming the same number of channels in the absence of NFA yields an open probability of p = 0.3% (Fig. 4F). The average open probability obtained by this method is p = 0.6 +/− 0.3% (n = 3; SEM) in the absence of NFA.

The dramatic increase of NFA potentiation and the very strong interaction seen with the F256A mutant suggest that the I–J loop may be involved in the NFA induced effects.

3.2. In CLC-K1 potentiation of F256A by NFA requires barttin

Unlike human CLC-Ks, rat CLC-K1 exhibits functional expression also without barttin [2,33]. Thus CLC-K1 is ideal to reveal possible barttin involvements in CLC-K regulation. CLC-K1/barttin [24] as well as CLC-K1 without barttin yields currents at 10 µM and 200 µM NFA that are about 80% and 45% of those recorded in control conditions (Fig. 5). We inserted the mutation F256A in the CLC-K1 background to test if this substitution could induce NFA potentiation also of this channel. F256A CLC-K1 with (Fig. 6A) and without barttin (Fig. 6B) shows functional expression levels and kinetics comparable with those of WT with and without barttin. Interestingly, the application of 10 µM NFA caused a transient potentiation of F256A CLC-K1/barttin (Fig. 6C), even though steady state currents were not increased. Thus the F256A mutation induces potentiation in the CLC-K1 background. Surprisingly, no potentiation was found when F256A CLC-K1 was expressed without barttin (Fig. 6D). As illustrated in Fig. 6C and D, we separated the transient potentiating effect of NFA and the blocking effect [24], with the results shown in Fig. 6E. The maximal potentiation is estimated around 1.9 fold. The apparent NFA blocking effect on F256A CLC-K1 is weakly more pronounced (K_D ~ 33 µM) than on F256A CLC-K1/barttin (K_D ~ 142 µM),

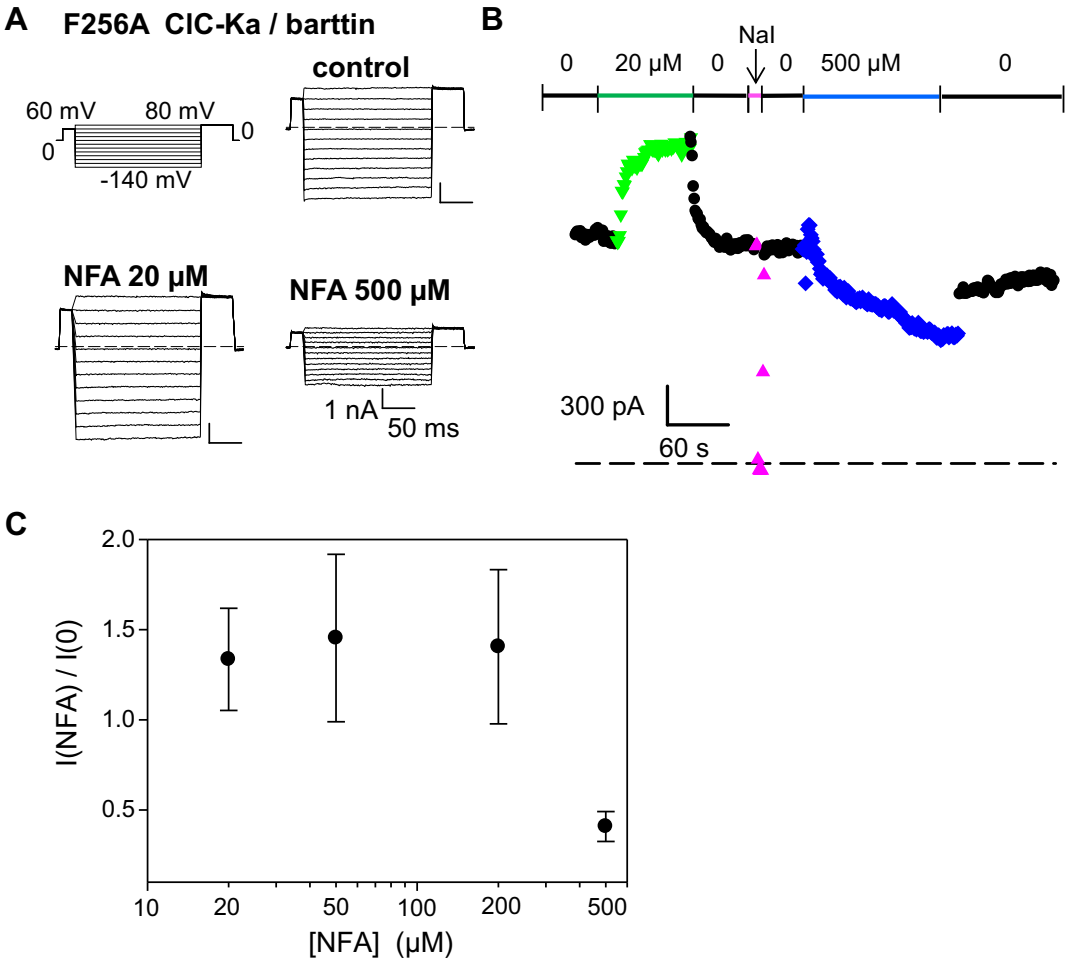

Fig. 7. NFA potentiation and block of F256A CLC-Ka in HEK293 cells. (A) Representative current recordings of F256A CLC-Ka/barttin expressed in HEK293 cells in control solution (top right), at 20 μM NFA (bottom left) and at 500 μM NFA (bottom right). (B and C) Effect of $[NFA]_{ext}$ on F256A CLC-Ka. (B) Mean current at 60 mV is plotted vs. time. Colors and symbols correspond to the $[NFA]_{ext}$ applied (0, 20, and 500 μM). (C) Normalized currents acquired at different $[NFA]_{ext}$ are plotted vs. $[NFA]_{ext}$ (used concentrations: 20, 50, 200, and 500 μM) ($n \geq 4$ for 20, 50, and 500 μM; $n = 17$ for 200 μM).

reflecting the overlap between potentiation and block seen in the CLC-K channels co-expressed with barttin. Thus this subunit participates in the pharmacological modulation of these channels.

3.3. The F256A mutation partially restores CLC-Ka biphasic response to NFA also in HEK cells

We had found that in HEK293 cells both human CLC-Ks and rat CLC-K1 were inhibited by NFA at all the concentrations tested (from 0.3 to 2000 μM) [26]. We asked whether F256A mutation might restore NFA potentiation of CLC-Ka in HEK293 cells. In HEK293 cells, the CLC-Ka F256A mutant was overall similar to WT (Fig. 7A top), showing no signs of time- or voltage-dependent relaxations, and differing thus markedly in behavior compared to *Xenopus* oocytes [26]. Noteworthy, F256A CLC-Ka currents increased at 20 μM NFA, whereas they were inhibited by 500 μM NFA (Fig. 7A, B). The dose–response of the effect of NFA confirmed the biphasic modulation of this mutant by NFA with potentiation at $[NFA]_{ext}$ up to 200 μM (slightly lower compared with that found in oocytes) and inhibition at higher $[NFA]_{ext}$ (Fig. 7C), reminiscent of the biphasic response to NFA found in oocytes [19] (Fig. 2C). These results further confirm the involvement of F256 in the CLC-K potentiation by NFA. However, the variability of the potentiation seen in cells (see error bars in Fig. 7C), but not in oocytes, indicates that this process depends on cellular factors that remain to be identified.

3.4. The N257A mutation hugely increases CLC-Ka inhibition by NFA

Also the residue adjacent to F256, N257, when mutated to Ala dramatically changed CLC-Ka's response to NFA. Unlike F256A, N257A CLC-Ka expressed in oocytes yields very large and voltage-independent currents (Fig. 8A, left). The response of this mutant to NFA was peculiar: even as low as 5 μM NFA induced ~90% inhibition (Fig. 8A right). In fact, N257A expressed in oocytes was only blocked at all $[NFA]_{ext}$ tested (from 1 to 2000 μM) with an apparent $K_D \sim 1$ μM (Fig. 8B). Interestingly, N257A currents continue to decrease after a brief application of NFA even if the drug is completely washed out (Fig. 8C, left). The final current level is almost as low as that achieved with a continuous application of NFA (Fig. 8C, right). Thus NFA binding does not cause immediate block but rather induces a conformational change resulting in channel closure.

To test if NFA block of N257A CLC-Ka reflects a reduction of the conductance or a reduced open probability, we first performed non-stationary noise analysis. However the lack of current kinetics of N257A CLC-Ka (Fig. 9A left and middle) only allowed us to resolve a restricted range of a putative parabola in the variance–mean plot rendering this approach unreliable (not shown). Thus, as a tool to introduce current relaxations, we used p-chlorophenoxy-acetic acid (CPA), that is known to block CLC-0 and CLC-1 currents at negative potentials inducing a closure of individual pore with only a small direct effect on the single channel conductance [29,34,35]. In fact, 100 μM CPA_{int} inhibits N257A CLC-Ka at negative voltages conferring to this mutant current

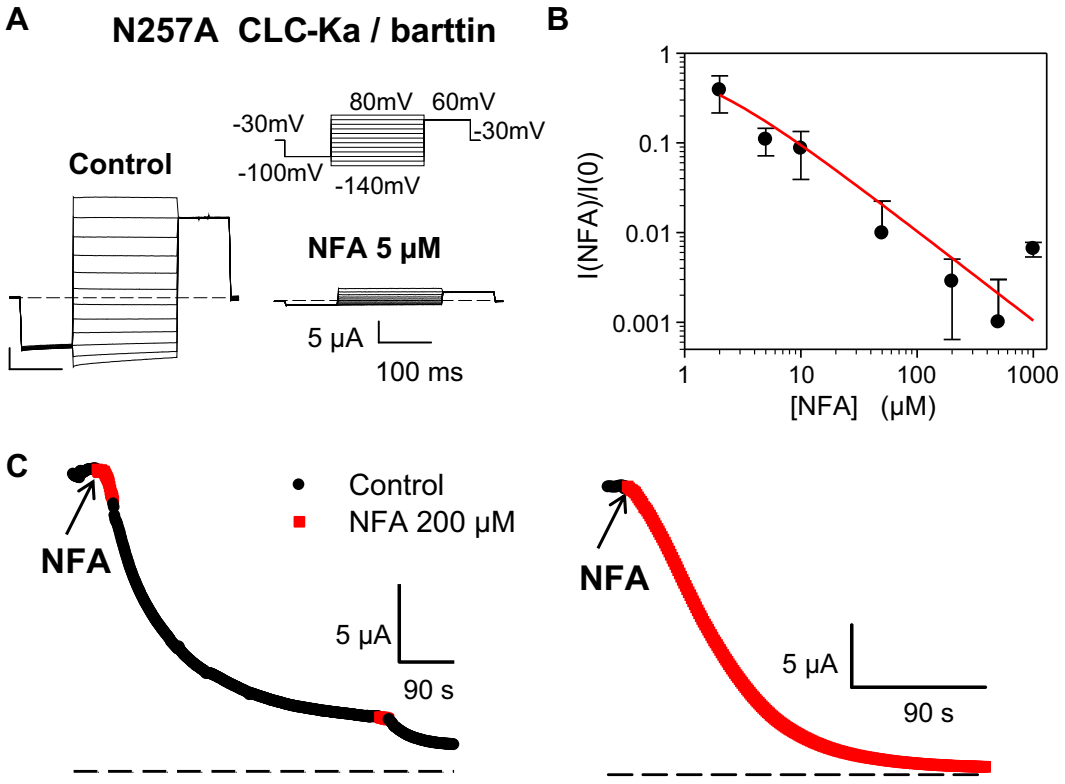

Fig. 8. Dramatic inhibition of N257A CLC-Ka by NFA. (A) Typical currents of N257A CLC-Ka expressed in *Xenopus* oocytes in control solution (left) and at 5 μM NFA (right). (B) Dose–response relationship of NFA effect on N257A CLC-Ka. Normalized currents are plotted vs. $[NFA]_{ext}$ (used concentrations: 2, 5, 10, 50, 200, 500, and 1000 μM) ($n \geq 4$ except $n = 3$ for 1000 μM). The red line represents the fit curve obtained from the equation $I / I_0 = 1 / (1 + (c / K_D))$ with $K_D \sim 1$ μM. (C) Insensitivity to washing of N257A CLC-Ka inhibition. Mean currents plotted as function of time after a short NFA perfusion (left) (similar experiments $n = 4$) or a longer NFA perfusion (right) (similar experiments $n = 10$). Colors and symbols represent the solutions applied.

kinetics (Fig. 9A, right) that are ideal for non-stationary noise analysis (Fig. 9B and C) and that resemble the fast protopore gate of CLC-0 [36]. This approach indicates that NFA does not affect the conductance of N257A (Fig. 9D). Interestingly, these values for N257A in the presence of CPA are ~32–42% of those obtained for F256A without CPA (Fig. 3D). Previously it was shown that in CLC-0 CPA induces a voltage-dependent closure of individual protopores of the gating glutamate E166A mutant, which lacks the regular fast gate [29,35]. Thus, the smaller conductance seen for N257A in the presence of CPA might either reflect a closure of the individual protopores or could be caused by a direct effect of the mutation on channel conductance. To distinguish between these hypotheses, we performed single channel measurements of N257A CLC-Ka with and without CPA (Fig. 10). In the absence of CPA, the mutant exhibits very slow gating kinetics and several conductive states (Fig. 10) that were not found for F256A, but which are of the same order of magnitude of the conductance of F256A (0.4 pA–1.9 pA) (Fig. 10B, C). Thus N257A mutation introduces a variability of the conductance levels rendering difficult to directly compare it with mutant F256A. In any case, we can conclude that the much higher level of functional expression of this mutant compared to WT does not reflect a substantial increase of the single channel conductance. In the presence of CPA, channel openings are much shorter (Fig. 10B, right) and the predominant conductance level has an amplitude of ~0.66 pA (Fig. 10C). Overall, the results from the single channel recordings are compatible with the non-stationary noise analysis. The overall channel activity indicates a relatively large open probability (Fig. 10) (~25% assuming two independent channels in the patch). However, the multiple conductance levels render a quantitative analysis difficult.

From the combined evidence from noise analysis and single channel recording, we can conclude that the mutation N257A by itself does not significantly change the single channel conductance, that the mutant has a large constitutive open-probability (compared to WT CLC-Ka), and that the inhibition of the mutant by NFA reflects a reduced open-probability, with unaltered channel conductance.

Next we tested the effect of NFA on N257A in CLC-K1. Unlike for CLC-Ka, the substitution of N257 with Ala did not modify magnitude and kinetics of CLC-K1 currents (Fig. 11). Moreover N257A CLC-K1 with or without barttin was only weakly more sensitive to NFA compared with WT (Fig. 11). Thus the high NFA affinity of N257A is a characteristic of CLC-Ka.

4. Discussion

Because of the causative association of CLC-K channels with Bartter syndrome and a proposed association with hypertension, several works aimed at a pharmacological characterization of these channels. Among the compounds identified, NFA was the most potent activator of hCLC-Ks expressed in *Xenopus* oocytes. Surprisingly, no NFA activation

Fig. 9. Non-stationary noise analysis of N257A CLC-Ka. (A) Typical patch clamp inside-out traces of N257A CLC-Ka measured from different oocytes in control conditions (left), at 4 μM NFA_{ext} (middle), at 4 μM NFA_{ext} and 100 μM CPA_{int} (right). (B and C) Examples of non-stationary noise analysis of N257A CLC-Ka in the presence of 100 μM CPA_{int}, in control external solution (B) and at 4 μM NFA_{ext} (C). Analysis was performed both for the deactivating currents at −100 mV as well as for the unblocking relaxations at 60 mV. The traces shown are an example at 60 mV (left). Mean currents (upper) and variance (lower) are shown as a function of time (right). Variance (symbols) is plotted versus the mean current and fitted with a parabola (red line) as described in the Materials and methods section. (D) Bars represent the absolute value of the single channel mean current in the presence of 100 μM CPA_{int} in external control solution and at 4 μM NFA_{ext} at two different potentials (−100 mV and 60 mV) ($n \geq 3$), $p > 0.3$ (unpaired Student's t-test) (background variance and leak currents were subtracted).

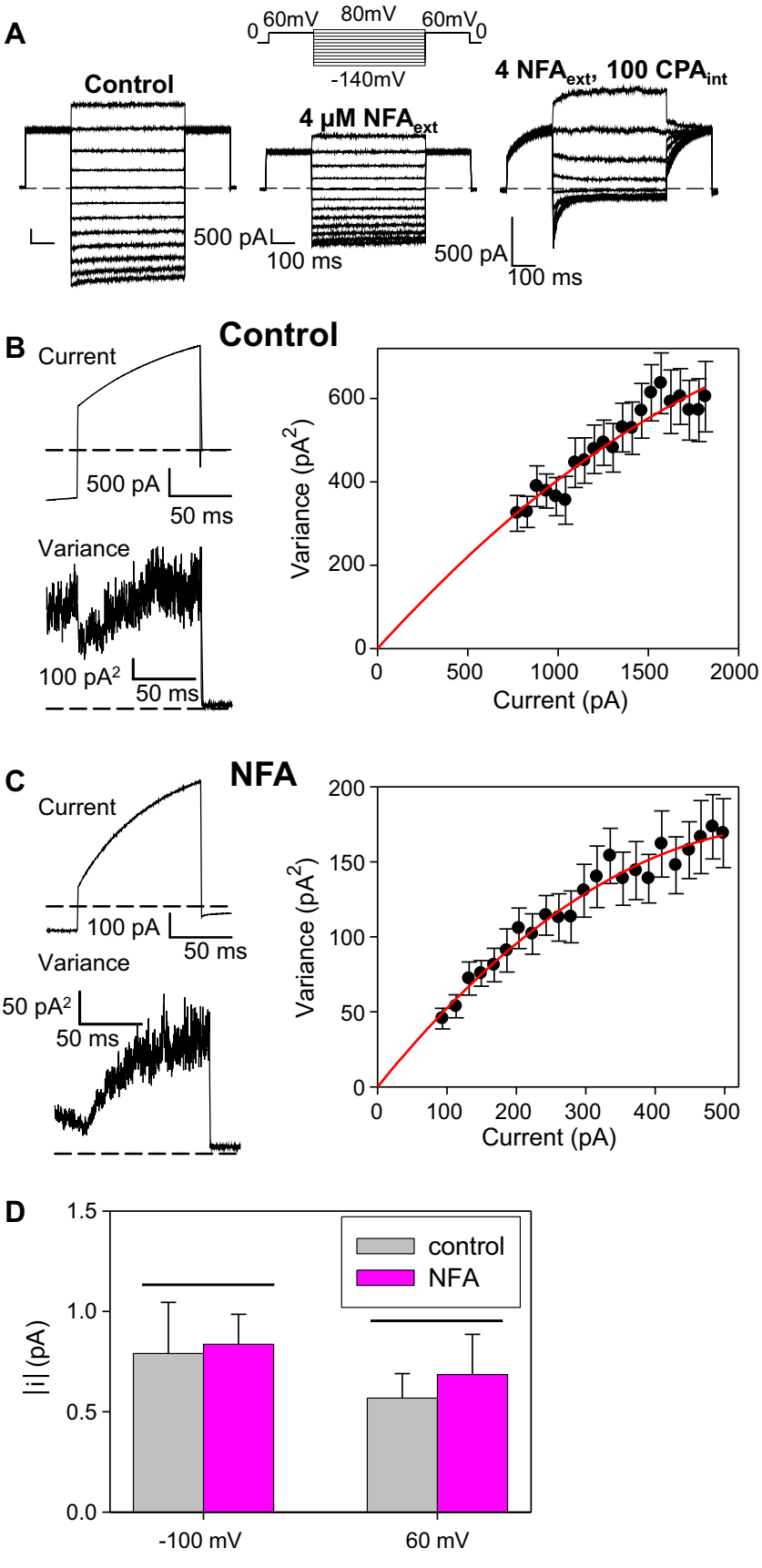
A
0 60mV 80mV 60mV 0
-140mV
Control
4 μM NFA$_{ext}$
4 NFA$_{ext}$, 100 CPA$_{int}$
500 pA
100 ms
500 pA
100 ms
B
Control
Current
500 pA
50 ms
Variance
100 pA^2
50 ms
Variance (pA^2)
Current (pA)
C
NFA
Current
100 pA
50 ms
Variance
50 pA^2
50 ms
Variance (pA^2)
Current (pA)
D
control
NFA
|i| (pA)
-100 mV
60 mV

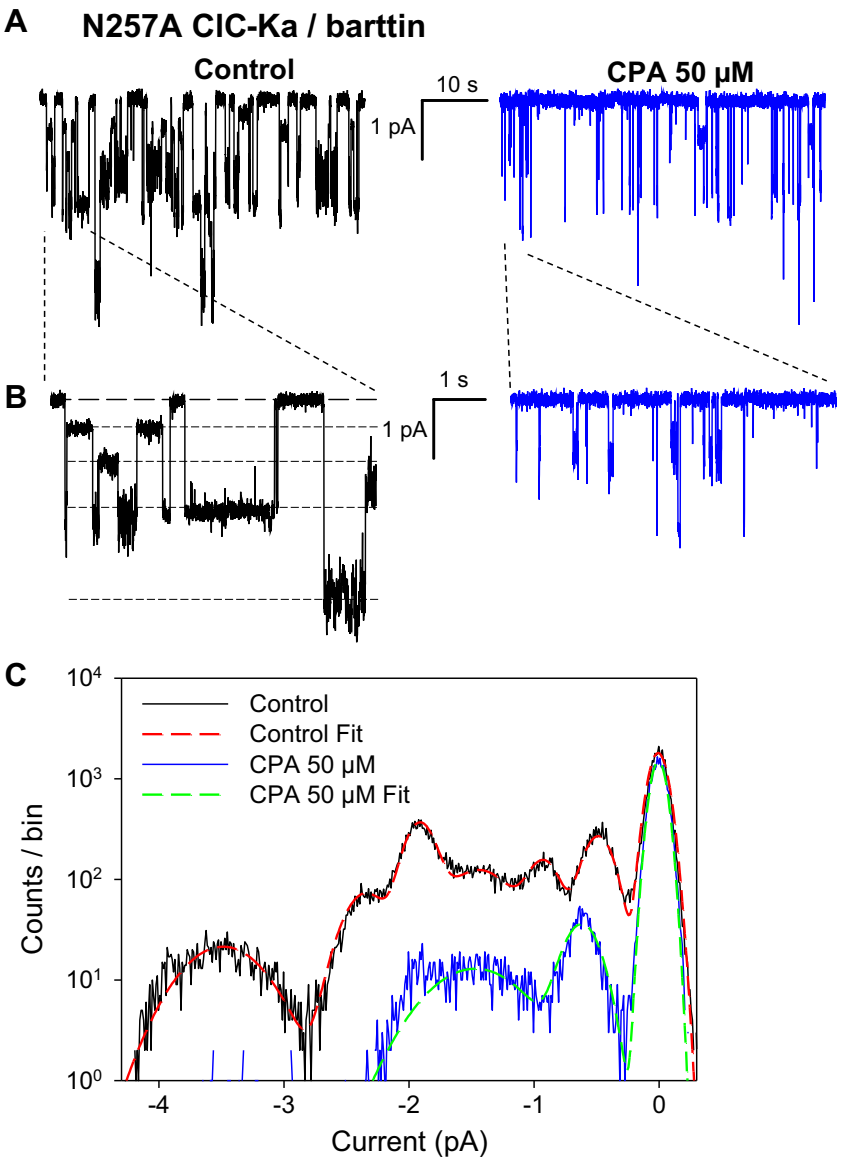

Fig. 10. Single channel recordings from N257A CLC-Ka. (A) Representative traces from a single patch at −100 mV in internal control solution and in 50 μM CPA (similar experiments n = 5). (B) Short stretches of the traces in (A) shown at a higher time resolution. In the left panel dashed lines indicate several distinct conductance levels. (C) Amplitude histogram of the recording at −100 mV in control solution and in the presence of 50 μM CPA. Dashed lines are fit curves superimposed. In the presence of CPA the dominant current level has an amplitude of 0.66 pA. There is no clear correspondence between the peaks in control and in CPA.

was seen when hCLC-Ks were expressed in mammalian cells [26], probably reflecting a near-maximal open probability of the channels in that expression system. Thus, here we further investigated the NFA activation of CLC-Ks in oocytes to identify molecular determinants of this process. We employed the CLC-Ka isoform because it shows much higher current expression in oocytes compared to CLC-Kb. Since both isoforms are potentiated by NFA by similar mechanisms, our findings are likely relevant for CLC-Kb as well.

We identified two adjacent residues belonging to the I–J loop, F256 and N257, that are involved in the CLC-K modulation by NFA. In *Xenopus* oocytes, F256A induces a huge NFA potentiation in CLC-Ka and a transient potentiation in CLC-K1, which is normally only blocked by NFA. Importantly, it partially recovers the biphasic response to NFA of CLC-Ka in HEK293 cells. Surprisingly, the CLC-Ka N257A mutant expressed in oocytes shows very large and voltage-independent currents, which are only blocked by NFA (K_D ~ 1 μM). By non-stationary noise analysis and single channel measurements we established that the potentiation of F256A and the inhibition of N257A by NFA reflect a change of the open probability of the channel, while NFA does not affect the single-channel conductance of these mutants. The single channel analysis confirmed that the open-probability of CLC-Ka in oocytes is extremely small (<1%). Interestingly, in the presence of NFA, the open-probability of mutant F256A CLC-Ka reaches values around 20%, becoming more similar to what is observed for the channel expressed in HEK cells [26].

Interestingly, the conductance estimated for F256A is similar to that of WT CLC-Ka [14,25] and roughly twice the value obtained for N257A from CPA induced current relaxations by non-stationary noise analysis. Regarding N257A, single channel recordings showed several conductance levels and much slower gating kinetics. We speculate that the flickery open single channel current of F256A (Fig. 4B, C) could be caused by the presence of various conductance levels, which are not temporally resolved, and that the mutant N257A slows down these fluctuations, resulting in well resolved conductance levels. Further experiments are needed to clarify this interesting detail. We cannot, however, rule out that mutant N257A directly alters the channel conductance, even though N257 is located far away from the channel pore.

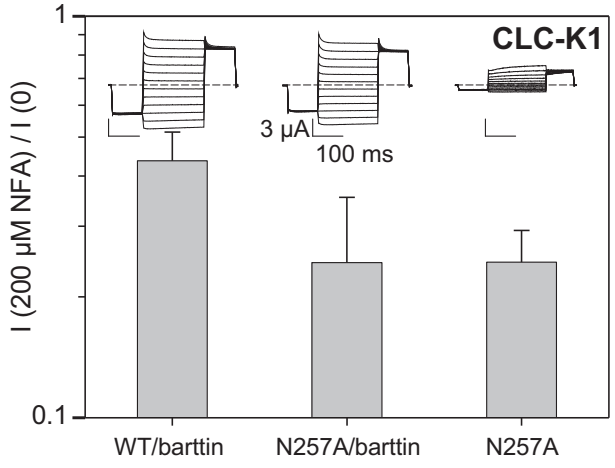

Fig. 11. NFA affinity of N257A CLC-K1 is comparable to that of WT CLC-K1. Comparison of normalized currents of WT CLC-K1/barttin (n = 5), N257A/barttin (n = 3), and N257A (n = 5) at 200 μM NFA normalized to the current recorded in control condition. On top of the figure typical current traces of WT/barttin, N257A/barttin, and N257A CLC-K1 (from left to right).

From our results we cannot conclude that F256 and N257 are directly involved in NFA binding, but we establish that the I–J loop harboring them is involved in the mechanism that underlies NFA potentiation. The NFA potentiation of F256A (and of WT CLC-Ka expressed in oocytes) clearly reflects a conformational change of the protein. The NFA binding site mediating the potentiation (site "P") is likely different from the binding site mediating block of CLC-K1, WT CLC-Ka, and all CLC-Ks in HEK293 cells (site "B") [24,26]. We believe that the dramatic block of N257A CLC-Ka is mediated by the normally potentiating site "P" and not by the regular blocking site "B". Indeed, block of N257A occurs with high affinity, as the potentiation of F256A and it involves a slow conformational change as evidenced by the continuous reduction of currents after washout (Fig. 8C).

Apart from pointing to a region that is involved in NFA potentiation the two mutants F256A and N257A teach us an important lesson. The fact that a relatively minor point mutation far away from the channel pore is able to hugely increase the open probability (p_{open}) of the channel, shows that p_{open} is a fragile property. Thus, the very large p_{open} of CLC-K channels expressed in HEK293 cells [10,11,26] compared to the small p_{open} in oocytes [14] might be caused by a relatively subtle difference between the two systems.

F256 and N257 as well as the extracellular Ca^{2+} binding site [23,27] belong to the I–J loop which has a peculiar role in the structure of CLC proteins [28]. Additionally, the residue responsible for acidic block of CLC-Ks, H497 [14], is positioned quite close to this loop. Our study shows that the I–J loop is important for the regulation of CLC-K channels by extracellular ligands. Thus, this loop may represent an ideal target for potential drugs aimed at the potentiation of CLC-K channels in their native environment.

Finally, we demonstrated that the barttin subunit is required for the NFA activation of CLC-K channels. Thus, in addition to barttin's known roles [5,10–12], it also participates in the pharmacological modulation of CLC-K channels. Thus, the different response to NFA of CLC-Ks expressed in HEK293 cells might depend on a different interaction channel/barttin in oocytes compared to mammalian cells. In conclusion, in this work we identified two suitable targets for drugs: the I–J loop of the channel and its barttin subunit.

Acknowledgements

We thank T.J. Jentsch for all WT clones and F. Quartino, A. Barbin, and D. Magliozzi for the technical assistance. This work was supported by Telethon Italy (grant GGP 12008 to M.P., GGP 10101 to D.C.C., and GEP 13101 to GZ) and the Italian Ministry of Education (progetto MIUR-COFIN-2009 to M.P. and D.C.C.).

References

[1] S. Kieferle, P. Fong, M. Bens, A. Vandewalle, T.J. Jentsch, Two highly homologous members of the ClC chloride channel family in both rat and human kidney, Proc. Natl. Acad. Sci. U. S. A. 91 (1994) 6943–6947.
[2] S. Uchida, S. Sasaki, T. Furukawa, M. Hiraoka, T. Imai, Y. Hirata, F. Marumo, Molecular cloning of a chloride channel that is regulated by dehydration and expressed predominantly in kidney medulla, J. Biol. Chem. 268 (1993) 3821–3824.
[3] S. L'Hoste, A. Diakov, O. Andrini, M. Genete, L. Pinelli, T. Grand, M. Keck, M. Paulais, L. Beck, C. Korbmacher, J. Teulon, S. Lourdel, Characterization of the mouse ClC-K1/Barttin chloride channel, Biochim. Biophys. Acta 1828 (2013) 2399–2409.
[4] S. Uchida, S. Sasaki, K. Nitta, K. Uchida, S. Horita, H. Nihei, F. Marumo, Localization and functional characterization of rat kidney-specific chloride channel, ClC-K1, J. Clin. Invest. 95 (1995) 104–113.
[5] R. Estévez, T. Boettger, V. Stein, R. Birkenhäger, E. Otto, F. Hildebrandt, T.J. Jentsch, Barttin is a Cl^- channel beta-subunit crucial for renal Cl^- reabsorption and inner ear K^+ secretion, Nature 414 (2001) 558–561.
[6] T.J. Jentsch, I. Neagoe, O. Scheel, CLC chloride channels and transporters, Curr. Opin. Neurobiol. 15 (2005) 319–325.
[7] G. Rickheit, H. Maier, N. Strenzke, C.E. Andreescu, C.I. De Zeeuw, A. Muenscher, A.A. Zdebik, T.J. Jentsch, Endocochlear potential depends on Cl(−) channels: mechanism underlying deafness in Bartter syndrome IV, EMBO J. 27 (2008) 2907–2917.
[8] A.A. Zdebik, P. Wangemann, T.J. Jentsch, Potassium ion movement in the inner ear: insights from genetic disease and mouse models, Physiology (Bethesda) 24 (2009) 307–316.
[9] R. Birkenhäger, E. Otto, M.J. Schurmann, M. Vollmer, E.M. Ruf, I. Maier-Lutz, F. Beekmann, A. Fekete, H. Omran, D. Feldmann, D.V. Milford, N. Jeck, M. Konrad, D. Landau, N.V. Knoers, C. Antignac, R. Sudbrak, A. Kispert, F. Hildebrandt, Mutation of BSND causes Bartter syndrome with sensorineural deafness and kidney failure, Nat. Genet. 29 (2001) 310–314.
[10] M. Fischer, A.G. Janssen, C. Fahlke, Barttin activates ClC-K channel function by modulating gating, J. Am. Soc. Nephrol. 21 (2010) 1281–1289.
[11] U. Scholl, S. Hebeisen, A.G. Janssen, G. Müller-Newen, A. Alekov, C. Fahlke, Barttin modulates trafficking and function of ClC-K channels, Proc. Natl. Acad. Sci. U. S. A. 103 (2006) 11411–11416.
[12] T. Stauber, S. Weinert, T.J. Jentsch, Cell biology and physiology of CLC chloride channels and transporters, Compr. Physiol. 2 (2012) 1701–1744.
[13] S. Waldegger, N. Jeck, P. Barth, M. Peters, H. Vitzthum, K. Wolf, A. Kurtz, M. Konrad, H.W. Seyberth, Barttin increases surface expression and changes current properties of ClC-K channels, Pflugers Arch. 444 (2002) 411–418.
[14] A. Gradogna, E. Babini, A. Picollo, M. Pusch, A regulatory calcium-binding site at the subunit interface of CLC-K kidney chloride channels, J. Gen. Physiol. 136 (2010) 311–323.
[15] A. Gradogna, M. Pusch, Alkaline pH block of CLC-K kidney chloride channels mediated by a pore lysine residue, Biophys. J. 105 (2013) 80–90.
[16] D.B. Simon, R.S. Bindra, T.A. Mansfield, C. Nelson-Williams, E. Mendonca, R. Stone, S. Schurman, A. Nayir, H. Alpay, A. Bakkaloglu, J. Rodriguez-Soriano, J.M. Morales, S.A. Sanjad, C.M. Taylor, D. Pilz, A. Brem, H. Trachtman, W. Griswold, G.A. Richard, E. John, R.P. Lifton, Mutations in the chloride channel gene, CLCNKB, cause Bartter's syndrome type III, Nat. Genet. 17 (1997) 171–178.
[17] C. Barlassina, C. Dal Fiume, C. Lanzani, P. Manunta, G. Guffanti, A. Ruello, G. Bianchi, L. Del Vecchio, F. Macciardi, D. Cusi, Common genetic variants and haplotypes in renal CLCNKA gene are associated to salt-sensitive hypertension, Hum. Mol. Genet. 16 (2007) 1630–1638.
[18] H. Sanada, J.E. Jones, P.A. Jose, Genetics of salt-sensitive hypertension, Curr. Hypertens. Rep. 13 (2011) 55–66.
[19] A. Liantonio, A. Picollo, E. Babini, G. Carbonara, G. Fracchiolla, F. Loiodice, V. Tortorella, M. Pusch, D.C. Camerino, Activation and inhibition of kidney CLC-K chloride channels by fenamates, Mol. Pharmacol. 69 (2006) 165–173.
[20] A. Liantonio, M. Pusch, A. Picollo, P. Guida, A. De Luca, S. Pierno, G. Fracchiolla, F. Loiodice, P. Tortorella, D. Conte Camerino, Investigations of pharmacologic properties of the renal CLC-K1 chloride channel co-expressed with barttin by the use of 2-(p-chlorophenoxy)propionic acid derivatives and other structurally unrelated chloride channels blockers, J. Am. Soc. Nephrol. 15 (2004) 13–20.
[21] K. Matulef, A.E. Howery, L. Tan, W.R. Kobertz, J.Du. Bois, M. Maduke, Discovery of potent CLC chloride channel inhibitors, ACS Chem. Biol. 3 (2008) 419–428.
[22] A. Picollo, A. Liantonio, M.P. Didonna, L. Elia, D.C. Camerino, M. Pusch, Molecular determinants of differential pore blocking of kidney CLC-K chloride channels, EMBO Rep. 5 (2004) 584–589.
[23] A. Gradogna, M. Pusch, Molecular pharmacology of kidney and inner ear CLC-K chloride channels, Front. Pharmacol. 1 (2010) 130.
[24] A. Picollo, A. Liantonio, E. Babini, D.C. Camerino, M. Pusch, Mechanism of interaction of niflumic acid with heterologously expressed kidney CLC-K chloride channels, J. Membr. Biol. 216 (2007) 73–82.
[25] G. Zifarelli, A. Liantonio, A. Gradogna, A. Picollo, G. Gramegna, M. De Bellis, A.R. Murgia, E. Babini, D.C. Camerino, M. Pusch, Identification of sites responsible for the potentiating effect of niflumic acid on ClC-Ka kidney chloride channels, Br. J. Pharmacol. 160 (2010) 1652–1661.
[26] P. Imbrici, A. Liantonio, A. Gradogna, M. Pusch, D.C. Camerino, Targeting kidney CLC-K channels: pharmacological profile in a human cell line versus Xenopus oocytes, Biochim. Biophys. Acta 1838 (2014) 2484–2491.

[27] A. Gradogna, C. Fenollar-Ferrer, L.R. Forrest, M. Pusch, Dissecting a regulatory calcium-binding site of CLC-K kidney chloride channels, J. Gen. Physiol. 140 (2012) 681–696.
[28] R. Dutzler, E.B. Campbell, M. Cadene, B.T. Chait, R. MacKinnon, X-ray structure of a ClC chloride channel at 3.0 Å reveals the molecular basis of anion selectivity, Nature 415 (2002) 287–294.
[29] A. Accardi, M. Pusch, Conformational changes in the pore of CLC-0, J. Gen. Physiol. 122 (2003) 277–293.
[30] S.H. Heinemann, F. Conti, Nonstationary noise analysis and application to patch clamp recordings, Methods Enzymol. 207 (1992) 131–148.
[31] M. Pusch, K. Steinmeyer, T.J. Jentsch, Low single channel conductance of the major skeletal muscle chloride channel, ClC-1, Biophys. J. 66 (1994) 149–152.
[32] U. Ludewig, M. Pusch, T.J. Jentsch, Independent gating of single pores in CLC-0 chloride channels, Biophys. J. 73 (1997) 789–797.
[33] S. Waldegger, T.J. Jentsch, Functional and structural analysis of ClC-K chloride channels involved in renal disease, J. Biol. Chem. 275 (2000) 24527–24533.
[34] R. Estévez, B.C. Schroeder, A. Accardi, T.J. Jentsch, M. Pusch, Conservation of chloride channel structure revealed by an inhibitor binding site in ClC-1, Neuron 38 (2003) 47–59.
[35] S. Traverso, L. Elia, M. Pusch, Gating competence of constitutively open CLC-0 mutants revealed by the interaction with a small organic inhibitor, J. Gen. Physiol. 122 (2003) 295–306.
[36] U. Ludewig, M. Pusch, T.J. Jentsch, Two physically distinct pores in the dimeric ClC-0 chloride channel, Nature 383 (1996) 340–343.